MHD Stagnation Point Flow and Heat Transfer of a Nanofluid Over a Stretching Sheet Fixed in Porous Medium with Effect of Thermal Radiation, Joule Heating and Heat Source/Sink

*R*avindra Kumar[1] *Ruchika Mehta*[1*], *Tripti Mehta*[2] *and Sushila*[3]
[1]*Department of Mathematics and Statistics*,
Manipal University Jaipur, Jaipur(Raj.), India
[1]*Department of Mathematics*,
Vivekananda Global University, Jaipur(Raj.), India
[2]*Department of Mathematics*,
S. S. Jain Subodh P. G. College, Jaipur(Raj.), India
[3]*Department of Physics*,
Vivekananda Global University, Jaipur(Raj.), India
ruchika.mehta1981@gmail.com

Abstract

The goal of this research is to see how thermal radiation, joule heating, and heat Source/Sink affect two-dimensional nanofluid stagnation point flow above a stretching sheet fixed in a spongy medium. This research accounts for the magnetic field, and the nonlinear Rosseland approximation is used to calculate heat radiation. The governing equations are converted into a system via similarity transformations in joined nonlinear ordinary differential equations, which are solved numerically using the Runge-Kutta fourth order approach with shooting technique. The numerical results reveal that this method has excellent correctness, good convergence with minimal computational cost, and a lot of promise. The velocity and temperature are also found to increase as a function of the radiation parameter, Eckert number, Brownian motion parameter, Thermophoresis parameter, Biot Number, and thermal buoyancy parameter, as well as the reverse effect in Prandtl numeral. The skin friction, local Nusselt number, and local Sherwood number are increasing functions of the ratio of free stream velocity to stretching sheet velocity parameter, Biot number, Brownian motion parameter, and thermophoresis parameter, with the reverse effect in magnetic parameter, Prandtl number, and permeability parameter.

Keywords: Nanofluid, Stretching Sheet, thermal radiation, joule heating, heat Source/Sink.

1 Introduction:

Nanofluid is a base fluid containing nanometer-sized particles/fibers (water, oil, ethylene glycol, etc.).Al_2O_3, Cu, T_iO_2, Ag, and other materials are commonly utilized for nanoparticles. These liquid combinations were discovered to have excellent assets that could make them useful in a variety of technical and manufacturing applications involving temperature transmission, nuclear reactors, petroleum cells, mi-

croelectronics, power production and carrying, space expertise, security and ships, and bony film solar power collectors are only few of the technologies that are being developed. [5] deals with (MHD) nanofluid stream towards a nonlinear extended plane with changeable depth in the company of an electric ground. In the existence of thermal radiation and Joule heating impacts, buoyant MHD nanofluid flow and heat transmission over a stretching sheet are examined [7]. [12] examined the impacts of thermally evolved thermophoresis diffusion and Brownian motion in non-Newtonian nanofluids across an angled extending sheet, as well as the belongings of hotness radiation and chemical response. [14]The influence of thermal radiation on a heat absorbing magneto-viscous nanofluid's dissipative boundary layer flow transversely a holey exponentially overextended pane with thermal slips and Navier's velocity was investigated. When there is a consistent magnetic field present. [15] Entropy generation study of a two-way nanofluid flick stream of Eyringâ€"Powell liquid with warmth and mass transport through an unstable porous stretched sheet was investigated (MHD). [21] The belongings of a magnetic ground and heat rays on the compelled convection stream of CuO-water nano-fluid transversely a stretched pane with a point of stagnation were statistically investigated. The effects of heat radiation on the heat transfer of water-based nanofluids containing exponentially stretched sheets of motile gyrotactic microorganisms were studied by [24]. [26] The authors presented a Form in mathematics for MHD radiative stream of III-grade nanomaterials limited by a nonlinear extending sheet of flexible thickness. [29] investigated the formation of entropy in a II-grade nanofluid MHD stream finished a sheet that is being heated convectively and using nonlinear current radioactivity and viscid .Numerous slip properties on MHD unsteady Maxwell nanofluid stream finished a holey overextended pane with thermal radioactivity and thermo-diffusion in the attendance of chemical response were examined by [1]. In the presence of thermal radiation and a heat source, a 2-way MHD stream of a Jeffery nanofluid transversely a stretched sheet has been quantitatively examined by [2]. In a 2-dimensional accepted convection stream of unstable electrical nanofluid with MHD across a linearly leaky stretched pane, the belongings of suction, as well as current radioactivity, and Joule heating, are investigated by [4]. [18] looked explored the influence of numerous slipups on axisymmetric (MHD) buoyant nano-fluid stream across an extending sheet.[20] The stream of a nanofluid with changeable liquid characteristics done an angled overextended pane in the existence of current energy and chemical response is investigated using unsteady magnetohydrodynamics (MHD). The impact of slip circumstances on the two-way unsteady varied convection stream of electric MHD nanofluid over a stretched sheet in the company of thermal energy, gluey debauchery, and chemical response are the subject of this research. [4]. The effect of nonlinear thermal radiation and spatial and temperature dependent heat generation/absorption on a 3- way MHD Jeffrey liquid stream across a nonlinearly With porous material present, a permeable stretched sheet was investigated. [10]. The current and Joule boiler effect of Casson nanofluid stream with chemical response across an inclined porous stretched surface is investigated in [11]. The effects of buoyancy force on viscoelastic (second grade fluid) magnetized nanofluid were studied by [13]. [19] using a stretched sheet immersed in a porous media generated by suction/blowing, researchers explored the belongings of viscous-Joule boiler, current energy, and warmth production (or absorption) on MHD nanofluid flow. [28] used the power of numerical computing-based Lobatto IIIA method to investigate warmth and mass transmission in 3-D MHD radioactive current of water-based mixture nanofluid across an extended sheet. [30] investigated the three-dimensional border coating stream of Maxwell nanofluid across a extending sheet using magnetohydrodynamic (MHD) warmth and mass transmission. [31] An unsteady magneto-hydrodynamic heat and mass transfer model is used to investigate the heat and mass transfer of a hybrid nanofluid flow across a stretched

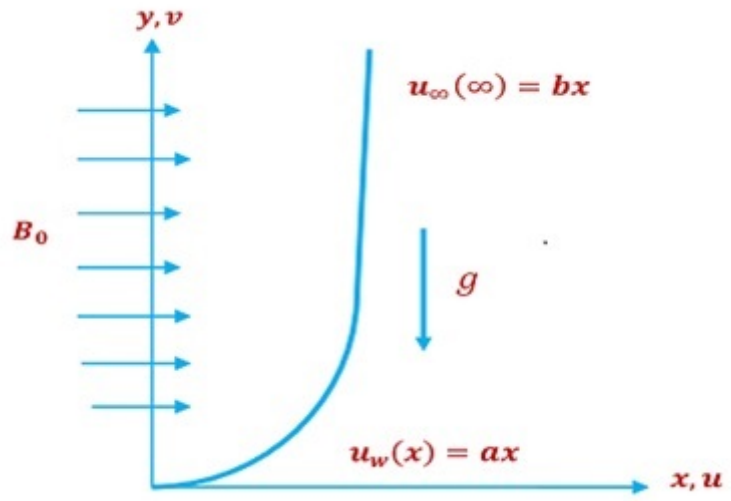

Figure 1: Schematic diagram of the Problem

surface. [32] investigated the heat and mass transfer characteristics of nanofluid flow over a stretched surface embedded in a porous medium in both steady and unsteady cases. [9] examined the effects of solar waves on 2-dimensional a stretched sheet is traversed by nanofluid stagnation-point flow. [16] looked at the heat transport and entropy of an unsteady flow of a non-Newtonian Casson nanofluid. [17] studied for magnetic dipole with stagnation point flow of micropolar nanofluids. [23] warmth and mass transport across a linear extending pane, as well as the essence of nonlinear thermal rays and entropy production for continuous laminar 2-way convective MHD Jeffrey nanofluid stream, were examined. [25]. The effects of convective boundary conditions on MHD Prandtl nanofluid flow over a stretched sheet were investigated.[3]considered the rheological and thermophysical characteristics of a non-Newtonian viscoelastic liquid under stratification over a linearly stretched surface.[27]This pagination's main goal is to outline characteristics of a water-based hybrid nanoliquid flow with single-wall carbon nanotube dispersion.

2 Construction of the Problem:

A steady nanofluid boundary layer flow in two dimensions through an extending sheet is using the speed of $u_w(x) = ax$ wherever a is a constant, as illustrated in Fig.1. A homogenous attractive arena of B_0 upright to the flow direction is supposed to be influenced. Warmth transmission scrutiny is done in the company of viscous dissipation and Joule heating and thermal energy qualities.T_w denotes the convective surface temperature which are based on Fig.1 and T_∞ symbolizes the ambient fluid temperature in the following governing equations. For this nano-fluid flow, the stable border line coat equations for stagnation point flow that is in-compressible:

$$\frac{\partial u}{\partial x} + \frac{\partial v}{\partial y} = 0, \tag{1}$$

$$u\frac{\partial u}{\partial x} + v\frac{\partial u}{\partial y} = u_\infty \frac{\partial u_\infty}{\partial x} + \nu\frac{\partial^2 u}{\partial y^2} - \frac{\sigma {B_0}^2 (u - u_\infty)}{\rho} - \frac{\nu}{k}(u - u_\infty) + g\beta_T(T - T_\infty) + g\beta_C(C - C_\infty), \tag{2}$$

Where u_∞ is the free stream velocity, ν means the kinematic viscocity, σ expressions forelectric conduction of liquid, B_0 establishes the unvarying magnetic arena along y-direction, k is used for porosity factor, u and v, respectively, stand for the x- and y-directional velocity components. We have the following border circumstances for the problem under consideration:

$$u = u_w(x) = ax, v = 0, at\ y = 0, and\ u \to u(\infty) = bx,\ \ as\ y \to \infty \tag{3}$$

The dimensionless variables are introduced in the form of

$$\eta = \sqrt{\frac{a}{\nu}} y\ , u = \frac{\partial \psi}{\partial y} = axf'(\eta)\ , v = -\frac{\partial \psi}{\partial x} = axf(\eta) \tag{4}$$

Eq. (1) is satisfied in the same way, and Eqs. (2) and (3) can be rewritten as

$$f''' + ff'' - {f'}^2 - \ (M + K)(f' - \lambda) + \lambda^2 + \lambda_1\theta + \lambda_2\phi = 0, \tag{5}$$

$$f(0) = 0,\ f'(0) = 1,\ when\ \eta = 0\ and\ f'(\infty) = \lambda,\ as\ \eta \to \infty, \tag{6}$$

where $M = \frac{(\sigma {B_0}^2)}{\rho a}$,is the magnetic restriction, $\lambda = \frac{b}{a}$, represents the share of the rates of unrestricted stream speed to the extending sheet speed, $K = \frac{\nu}{ka}$ is the permeability parameter $\lambda_1 = \frac{G_r}{R_e^2}$ is the thermal buoyancy parameter, where $G_r = g\beta_T(T_w - T_\infty)\frac{x^3}{\nu^2}$ is Grashof numeral, and $Re = \frac{(xU_w)}{\nu}$ is Reynolds number, $\lambda_2 = g\beta_C(C_w - C_\infty)\frac{x^3}{\nu^2}$ is the concentration buoyancy parameter.
Equation of Energy

$$\begin{aligned} u\frac{\partial T}{\partial x} + v\frac{\partial T}{\partial y} = \alpha\frac{\partial^2 T}{\partial y^2} + \frac{\nu}{C_p}(\frac{\partial u}{\partial y})^2 - \frac{1}{\rho c_p}\frac{\partial q_r}{\partial y} + \frac{\sigma {B_0}^2(u - u_\infty)^2}{\rho c_p} \\ +\tau(D_b\frac{\partial T}{\partial y}\frac{\partial C}{\partial y} + \frac{D_T}{T_\infty}(\frac{\partial T}{\partial y})^2) + \frac{Q^*(T - T_\infty)}{\rho c_p} \end{aligned} \tag{7}$$

Equation of Concentration

$$u\frac{\partial C}{\partial x} + v\frac{\partial C}{\partial y} = D_b\frac{\partial^2 C}{\partial y^2} + \frac{D_T}{T_\infty}(\frac{\partial T}{\partial y})^2 \tag{8}$$

where T symbolizes the temperature, C symbolizes the nanoparticles concentration, α is the current diffusivity, D_b and D_T are the Brownian motion coefficient and the thermophoretic dispersal coefficient, correspondingly. $\tau = \frac{(\rho p)_p}{(\rho p)_f}$ is the share of the nanoparticle active warmth size to the base fluid warmth size and q_r states to the radiative warmth flux amount. The radiative heat flux can be calculated using the Rosseland guess for current radiation and applied to optically thick medium as. $q_r = -\frac{4}{3}\frac{\sigma^*}{K^*}\frac{\partial T^4}{\partial y}$ where σ^*, k^* are the Stefan-Boltzman constant and average assimilation coefficient, correspondingly. $T^4 = 4T{T_\infty}^3 - 3T_\infty^4$ is achieved by utilising the Taylor series to expand $T^4$with respect to T_∞while disregarding terms of higher orders. As a result, Eq. (7) is found to be

$$\begin{aligned} u\frac{\partial T}{\partial x} + v\frac{\partial T}{\partial y} = \alpha\frac{\partial^2 T}{\partial y^2} + \frac{\nu}{C_p}(\frac{\partial u}{\partial y})^2 + \frac{16\sigma^* T_\infty^3}{3\rho C_p k^*}\frac{\partial^2 T}{\partial y^2} + \frac{\sigma {B_0}^2(u - u_\infty)^2}{\rho c_p} \\ +\tau(D_b\frac{\partial T}{\partial y}\frac{\partial C}{\partial y} + \frac{D_T}{T_\infty}(\frac{\partial T}{\partial y})^2) + \frac{Q^*(T - T_\infty)}{\rho c_p} \end{aligned} \tag{9}$$

For radiative heat flux modelling, the nonlinear Rosseland guess is used. As an outcome, the relevant convective warmth transport boundary conditions can be presented as.

$$-k\frac{\partial T}{\partial y} = (T - T_W), C = C_w, at\ y = 0, T \to T_\infty,\ C \to C_\infty, as\ \ y \to \infty \tag{10}$$

As a result of specifying the non-dimensional temperature $T = T_\infty + (T_w - T_\infty)\theta(\eta)$ and $C = C_\infty + (C_w - C_\infty)\phi(\eta)$. Eqs. (7) and (8) take the following format:

$$(1 + R_a)\theta^{''} + P_r[f\theta^{'} + ME_c(f^{'} - \lambda)^2 + E_c(f^{''})^2 + (N_b\theta^{'}\phi^{'} + N_t\theta^{'^2}) + \delta\theta\ ] = 0 \tag{11}$$

$$\phi^{''} + L_e f\phi^{'} + \frac{N_t}{N_b}\theta^{''} = 0, \tag{12}$$

and the borderline circumstances

$$\theta^{'}(0) = -(1 - \theta(0))Bi, \phi(0) = 1, \theta(+\infty) \to 0, \phi(+\infty) \to (0), \tag{13}$$

Where $P_r = \frac{\nu}{\alpha}$, is Prandtl number, $R_a = \frac{16\sigma^* T_\infty^3}{3kk^*}$, is radiation parameter, $E_c = \frac{U_w^2}{C_p(T_w - T_\infty)}$, is the Eckert number, $N_b = \frac{\tau D_b(C_W - C_\infty)}{\nu}$,shows the Brownian motion restriction, $N_t = \frac{\tau D_T(T_W - T_\infty)}{\nu T_\infty}$, is thermophoresis restriction,$\delta = \frac{Q^* L}{\rho C_p U_w}$, heat source/sink restriction, $L_e = \dfrac{\nu}{D_b}$, Lewis factor, $Bi = \dfrac{h}{k}\sqrt{\frac{\nu}{a}}$, denotes the Biot number. The three physical measures of our attention are the coefficient of skin friction C_{f_x}, the local Nusselt numberN_{u_x}, and local Sherwood number S_{u_x}, are given as.

$$C_{f_x} = \frac{\tau_w}{\rho U_w^2}, N_{u_x} = \frac{xq_w}{k(T_w - T_\infty)}, S_{u_x} = \frac{xq_m}{D_b(C_w - C_\infty)}, \tag{14}$$

where

$$\tau_w = \mu(\frac{\partial u}{\partial y})_{y=0}, q_w = -k(\frac{\partial T}{\partial y})_{y=0} + (q_r)_{y=0}, q_m = -D_b(\frac{\partial C}{\partial y})_{y=0}, \tag{15}$$

the relations will be.

$$C_{f_x}(R_e)^{\frac{1}{2}} = f^{''}(0),\ N_{u_x}(R_e)^{\frac{-1}{2}} = -(1 + R_a)\theta'(0), S_{u_x}(R_e)^{\frac{1}{2}} = -\phi^{'}(0), \tag{16}$$

The result of equations (4), (11) and (12) jointly through borderline circumstances (5) and (13) is determine through by a systematic numerical method called shooting technique. We translate the nonlinear equivalences into first order regular differential equivalences by labelling the variable quantity i.e.

$f = f_1, f^{'} = f_2, f^{''} = f_3, f^{'''} = f_3^{'}, \theta = f_4, \theta^{'} = f_5, \theta^{''} = f_5', \phi = f_6,$

$\phi^{'} = f_7, \phi^{''} = f_7^{'},$ Hence, the system of equations becomes

$$f_1^{'} = f_2, f_2^{'} = f_3, f_3^{'} = [f_2^2 - f_1 f_3 + (M + K)(f_2 - \lambda) - \lambda^2 - \lambda_1 f_4 - \lambda_1 f_6] \tag{17}$$

$$f_4^{'} = f_5, \tag{18}$$

$$f_5^{'} = -(1 + R_a)^{-1} P_r[f_1 f_5 + ME_c(f_2 - \lambda)^2 + E_c f_3^2 + N_b f_5 f_7 + N_t f_5^2 + \delta f_4] \tag{19}$$

$$f_6^{'} = f_7, \tag{20}$$

$$f_7^{'} = -(l_e f_1 f_5 + \frac{N_t}{N_b} f_5^{'}), \tag{21}$$

Subject to the following conditions

$$\begin{gathered} f_1(0) = 0, f_2(0) = 1, f_3(0) = S_1, f_4(0) = (1 + \frac{S_2}{B_i}), f_5(0) = S_2, f_6(0) = 1, \\ f_7(0) = S_3, \ as \ \eta \to 0 \ and \ f_2(\infty) = \lambda, f_4(\infty) = 0, f_6(\infty) = 0, \ as \ \eta \to \infty \end{gathered} \tag{22}$$

Now fourth order Runge-Kutta way with shooting technique is follow for stepwise integration and calculations are passed out on MATLAB computer software.

3 Influence of Diverse Restrictions

Ordinary differential equations that are nonlinear. (4), (11) and (12) are numerically solved with the borderline circumstances (5) and (13) using the MATLAB software and the shooting and fourth-order Runga-Kutta method. The obtained results demonstrate the impact of non-dimensional controlling parameters, specifically the magnetic field parameter M, Prandtl numeral P_r, radiation restriction R_a, the proportion of the free stream speed to the extending sheet speed restriction λ, Eckert numeral E_c, Thermophoresis restriction N_t, Brownian motion restriction N_b, Biot Numeral B_i, Lewis factor L_e, Permeability restriction K, thermal buoyancy parameter λ_1, Solutal buoyancy parameter λ_2 and Heat Source/Sink δ. Figures 2 and 3 depict the effect of the magnetic field restriction M on the velocity and temperature field distributions.It's worth noting that when M gets higher, the velocity field gets smaller. A resistive sort of force termed Lorentz force is created in the stream when the magnetic field parameter increases, causing a decrease in velocity field curves. It has been pragmatic that an enhance in magnetic parameters raises the temperature. The Lorentz force causes some additional warmth to be created in the flow. When the magnetic field is increased, the momentum layer thickness decreases while the thermal layer thickness increases. The impact of Prandtl number P_r on the supply of speed and temperature ground is exposed in Fig.4 and 5. It is perceived that growing values of P_r results a decline in velocity and temperature field. Figure 6 and 7 exhibits the significance of the radiation parameter R_a on the velocity and temperature, correspondingly. Figures 6 and 7 show that increasing the radiation parameter increases fluid velocity and temperature. The impact of proportion of the free stream speed to the speed of the extending sheet restriction λ on temperature arena is exposed in Fig.9. escalating values of Λ results a decrement in temperature field. The impact of Eckert number E_c, Brownian motion parameter N_b, Thermophoresis parameter N_t, Biot Numeral B_i on the sharing of speed and warmth field is exposed in Fig. 10, 11, 12, 13, 14, 15 16 and 17It has been observed that rising values of E_c, N_b, N_t and B_i results increment in velocity and temperature field.

4 Conclusions

The influence of thermal radiation, Heat Source/Sink, and joule heating on two-dimensional nanofluid stagnation point stream across a extending pane fixed in porous medium is discussed in this study. The controlling PDEs are changed into nonlinear ODEs using similarity transformations, and then These equations are numerically solved . The effects of a variety of non-dimensional characteristics on velocity and temperature fields are discussed and represented using graphs. The

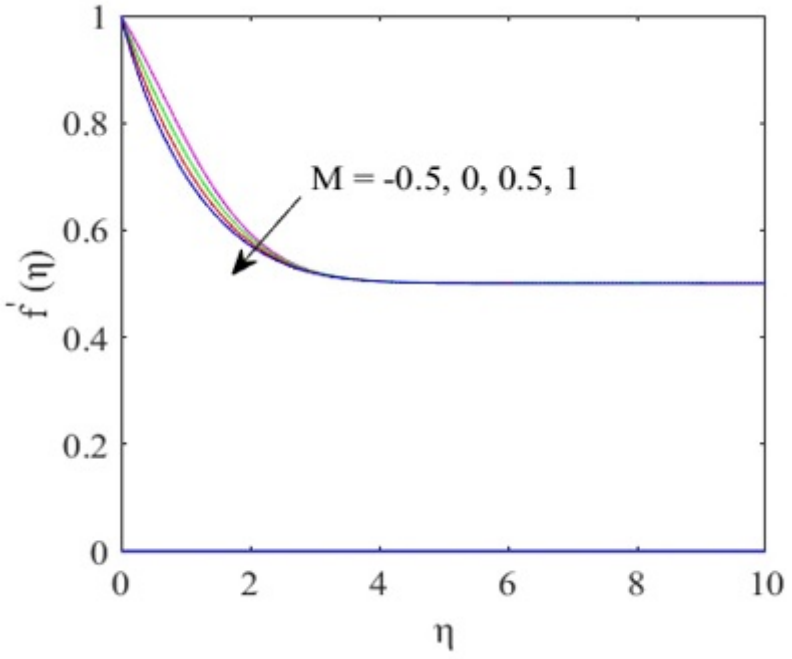

Figure 2: Velocity with η for disparate facts of magnetic restriction M.

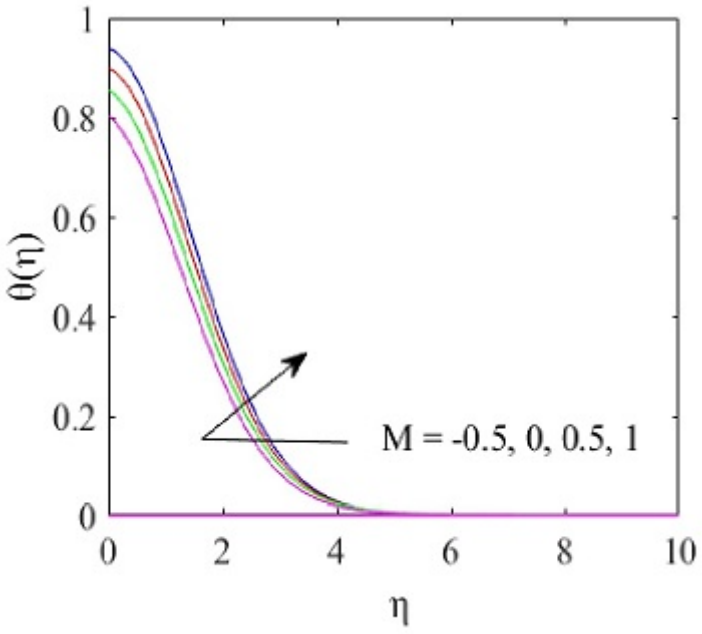

Figure 3: Temperature with η for disparate facts of magnetic restriction M.

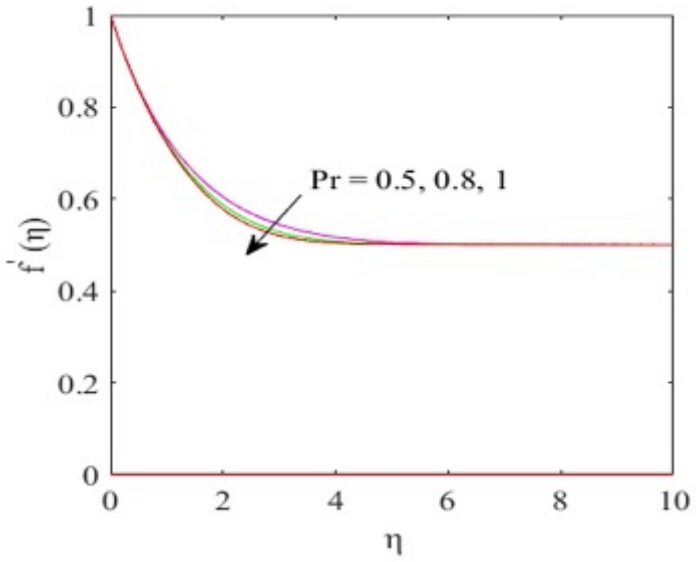

Figure 4: Velocity with η for disparate facts of Prandtl numeral P_r.

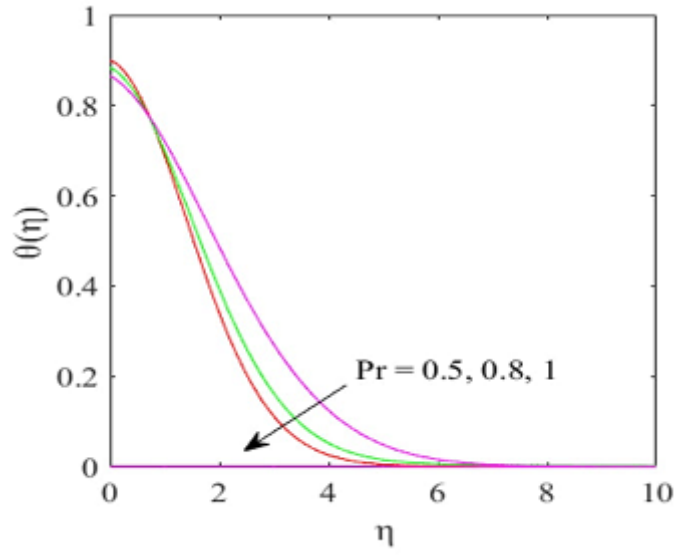

Figure 5: Temperature with η for disparate facts of Prandtl numeral P_r.

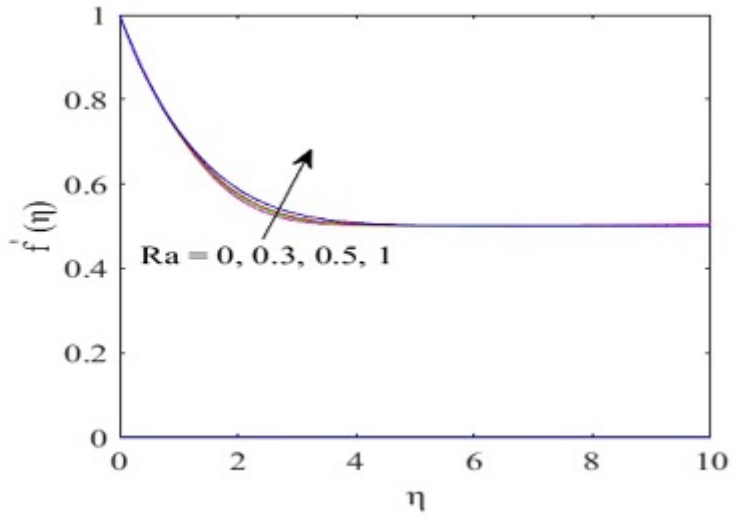

Figure 6: Velocity with η for disparate facts of radiation restriction R_a.

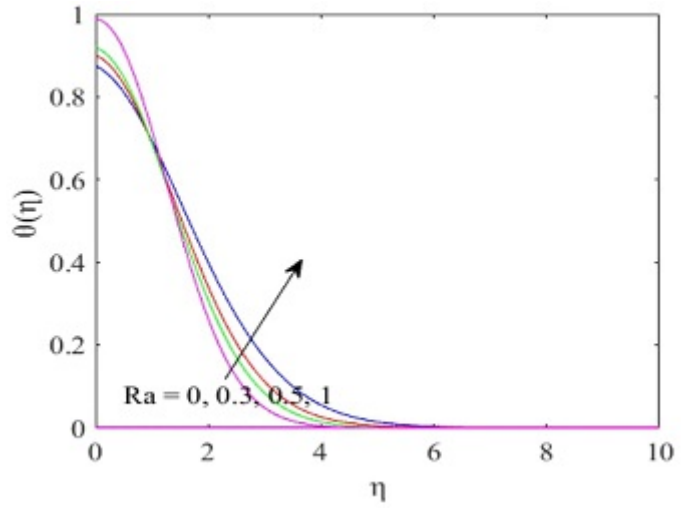

Figure 7: Temperature with η for disparate facts of radiation restriction R_a.

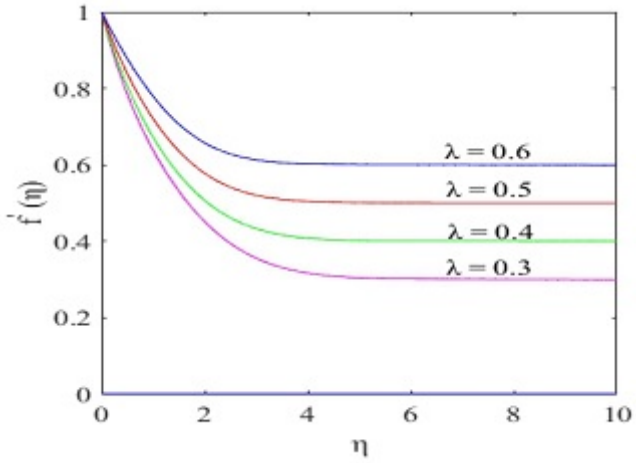

Figure 8: Velocity with η for disparate facts of free stream velocity to stretch sheet restriction velocity ratio of the stretching sheet parameter λ.

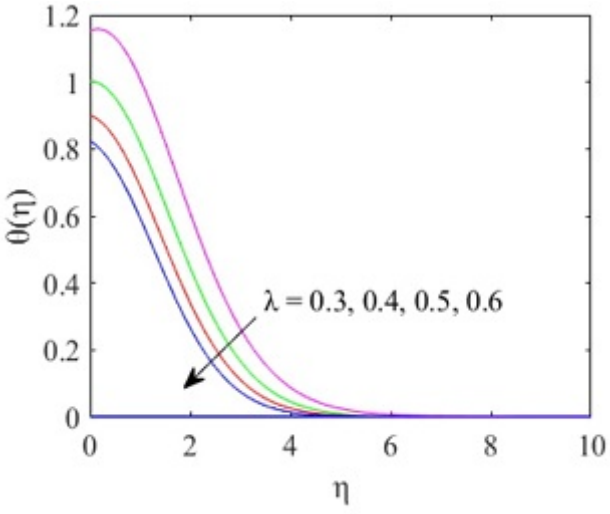

Figure 9: Temperature $\theta(\eta)$ related to η for unlike facts of ratio of the free stream velocity to stretch sheet restriction velocity ratio parameter λ.

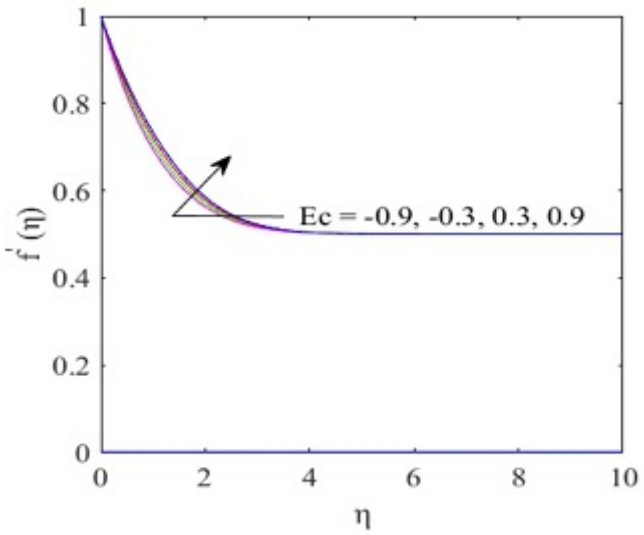

Figure 10: Velocity with η for disparate facts of Eckert numeral E_c.

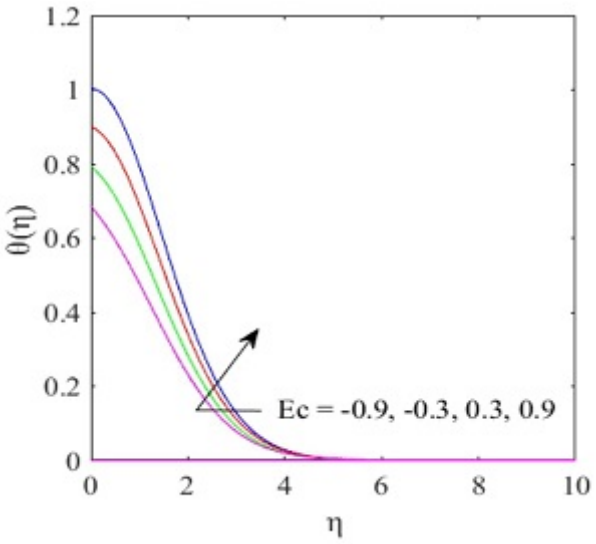

Figure 11: Temperature with η for disparate facts of Eckert numeral E_c.

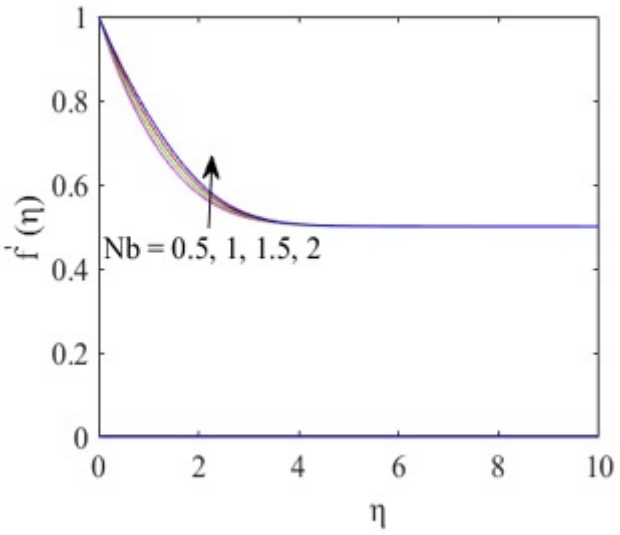

Figure 12: Velocity with η for disparate facts of Brownian motion parameter N_b.

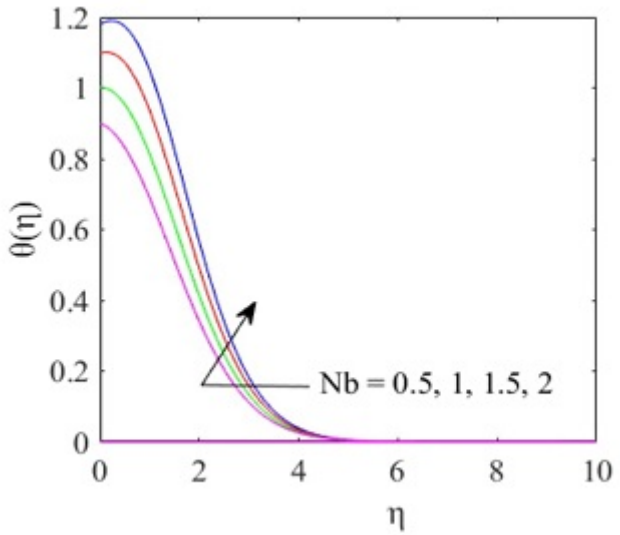

Figure 13: Temperature with η for disparate facts of Brownian motion parameter N_b.

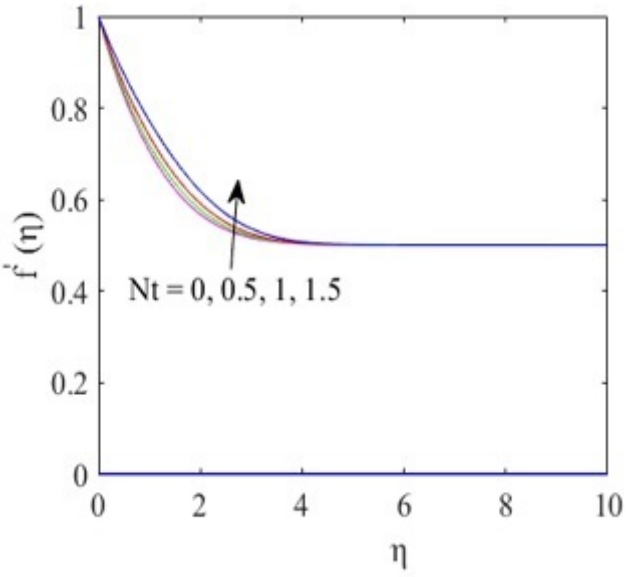

Figure 14: Velocity with η for disparate facts of Thermophoresis parameter N_t.

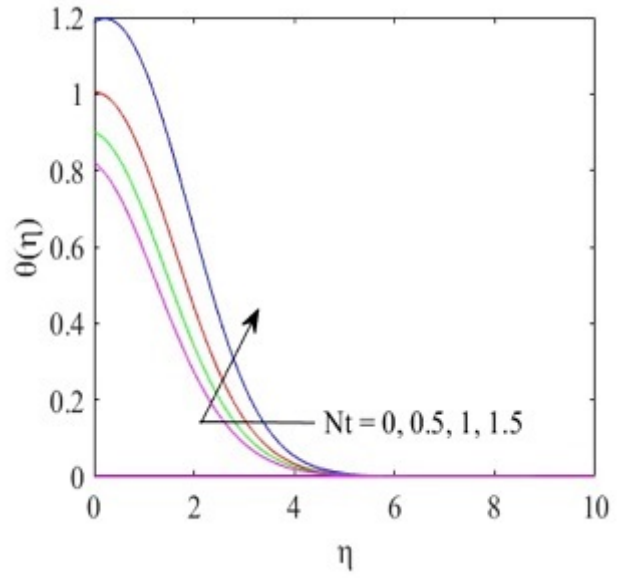

Figure 15: Temperature with η for disparate facts of Thermophoresis parameter N_t.

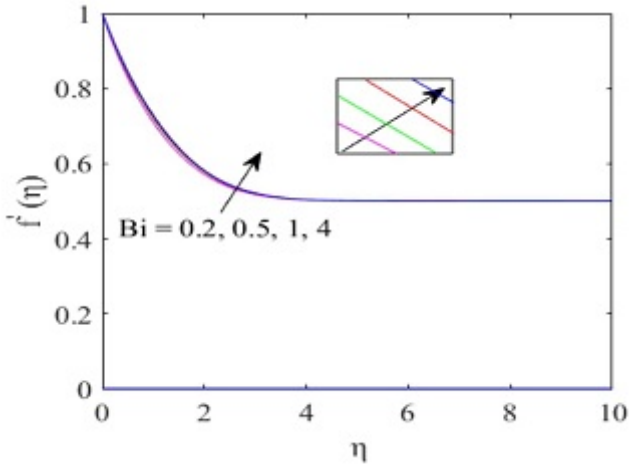

Figure 16: Velocity with η for disparate facts of Biot Numeral Bi.

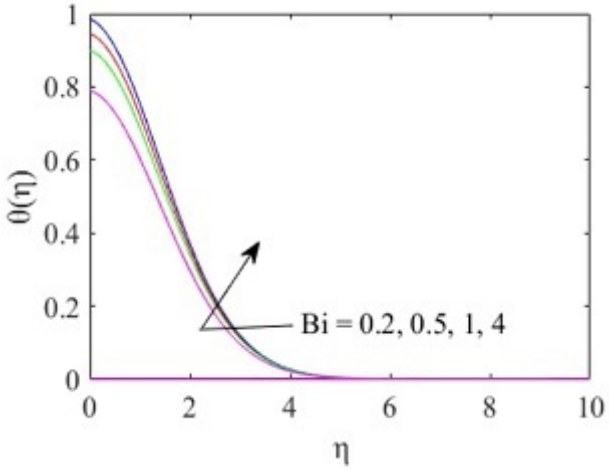

Figure 17: Temperature with η for disparate facts of Biot Numeral Bi.

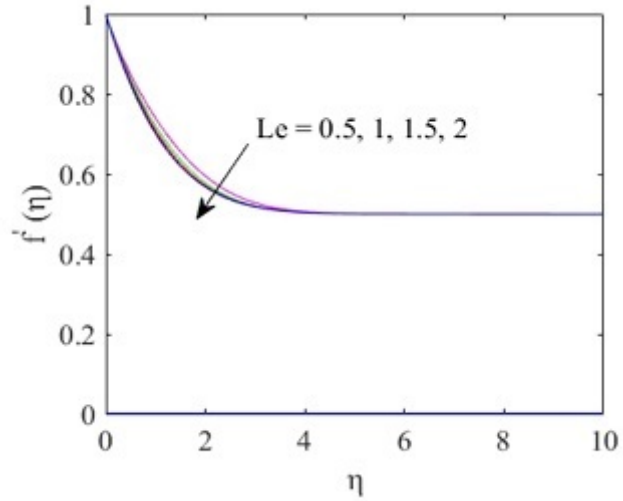

Figure 18: Velocity with η for disparate facts of Lewis factor L_e.

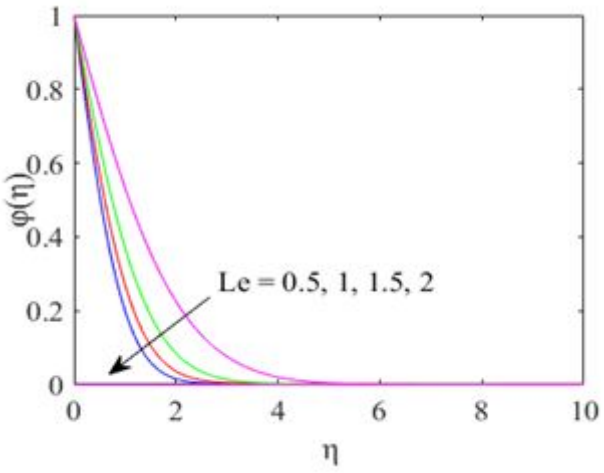

Figure 19: Concentration with η for disparate facts of Lewis factor L_e.

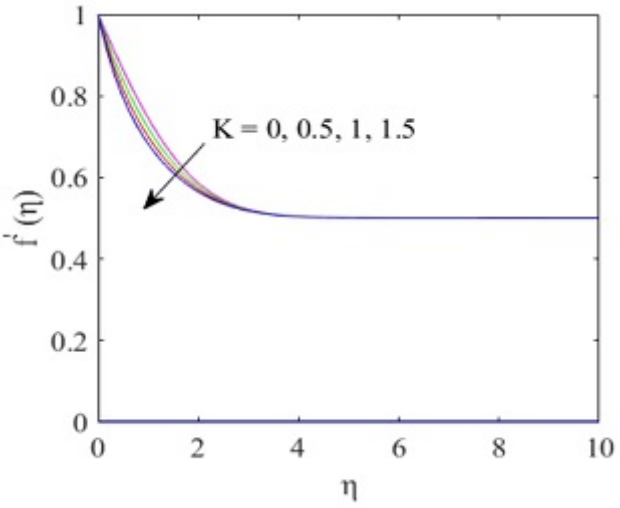

Figure 20: Velocity with η for disparate facts about permeability limitations K.

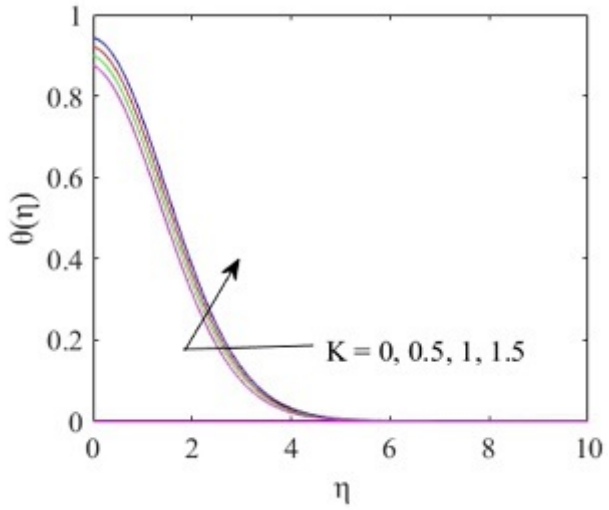

Figure 21: Temperature with η for disparate facts about permeability limitations K.

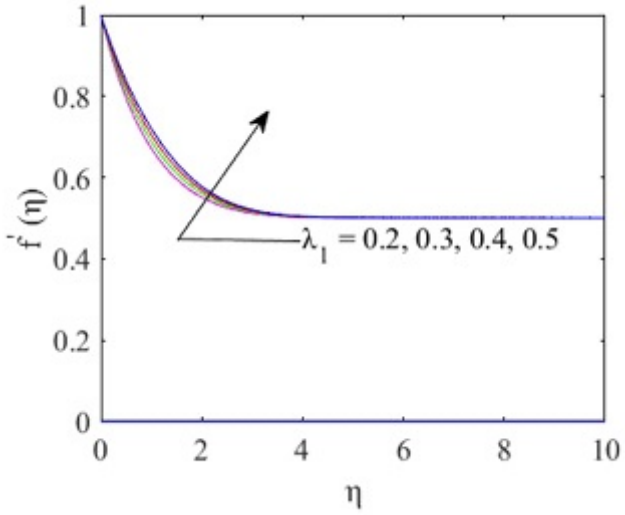

Figure 22: Velocity with η for disparate facts of thermal buoyancy parameter λ_1.

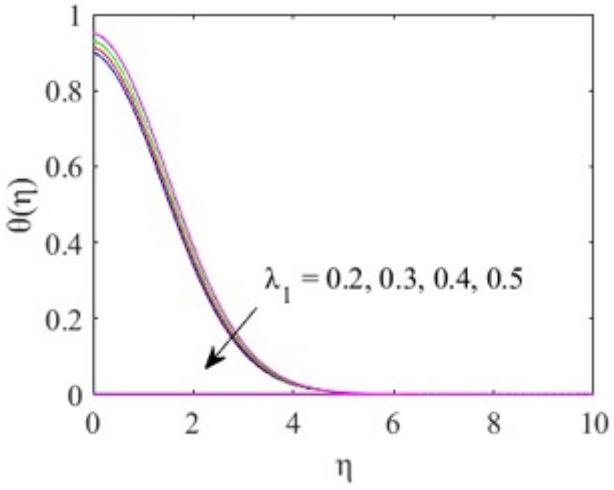

Figure 23: Temperature with η for disparate facts of thermal buoyancy parameter λ_1.

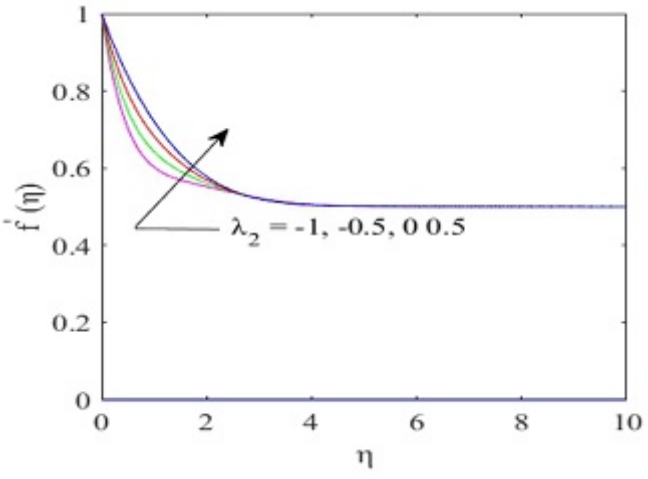

Figure 24: Velocity with η for disparate facts of Solutal buoyancy parameter λ_2.

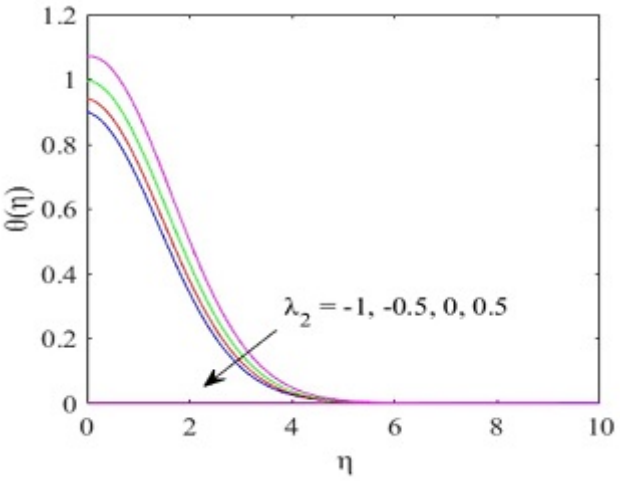

Figure 25: Temperature with η for disparate facts of Solutal buoyancy restriction λ_2.

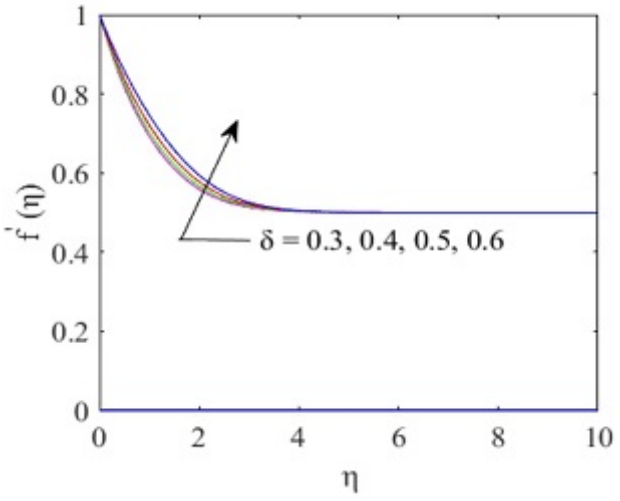

Figure 26: Velocity with η for disparate facts of Heat Source/Sink δ.

Table 1: Encouragement of the three physical dealings are the coefficient of skin friction C_{f_x}, the local Nusselt number N_{u_x} and local Sherwood number S_{u_x}.

Parameter	C_{f_x}	N_{u_x}	S_{u_x}
$M = -0.5$	-0.1951	0.1470	0.7460
$M = 0$	-0.2948	0.1080	0.7365
$M = 0.5$	-0.3866	0.0749	0.7291
$M = 1$	-0.4707	0.0450	0.7222
$P_r = 0.5$	-0.3827	0.1008	0.7316
$P_r = 0.8$	-0.3861	0.0870	0.7296
$P_r = 1$	-0.3866	0.0749	0.7291
$K = 0$	-0.2887	0.0930	0.7381
$K = 0.5$	-0.3866	0.0749	0.7291
$K = 1$	-0.4758	0.0585	0.7217
$K = 1.5$	-0.5573	0.0422	0.7160
$\lambda = 0.3$	-0.5386	-0.1136	0.7041
$\lambda = 0.4$	-0.4778	-0.0015	0.7141
$\lambda = 0.5$	-0.3866	0.0749	0.7291
$\lambda = 0.6$	-0.2743	0.1320	0.7460
$B_i = 0.2$	-0.4161	0.0630	0.7261
$B_i = 0.5$	-0.3866	0.0749	0.7291
$B_i = 1$	-0.3749	0.0813	0.7315
$B_i = 4$	-0.3641	0.0850	0.7326
$\lambda_1 = 0.2$	-0.5240	0.0369	0.7145
$\lambda_1 = 0.3$	-0.4762	0.0518	0.7196
$\lambda_1 = 0.4$	-0.4307	0.0642	0.7251
$\lambda_1 = 0.5$	-0.3866	0.0749	0.7291
$\lambda_2 = -1$	-0.9295	-0.0525	0.6858
$\lambda_2 = -0.5$	-0.7493	0.0030	0.7006
$\lambda_2 = 0.5$	-0.3866	0.0749	0.7291
$E_c = -0.9$	-0.4532	0.2360	0.7191
$E_c = -0.3$	-0.4204	0.1557	0.7241
$E_c = 0.3$	-0.3866	0.0749	0.7291
$E_c = 0.9$	-0.3546	-0.0021	0.7352
$\delta = 0.3$	-0.4505	0.2182	0.7189
$\delta = 0.4$	-0.4241	0.1590	0.7231
$\delta = 0.5$	-0.3866	0.0749	0.7291
$\delta = 0.6$	-0.3283	-0.0563	0.7391
$N_b = 0.5$	-0.3866	0.0749	0.7291
$N_b = 1$	-0.3519	-0.0014	0.7335
$N_b = 1.5$	-0.3180	-0.0732	0.7375
$N_b = 2$	-0.2880	-0.1344	0.7406
$N_t = 0$	-0.4150	0.1347	0.7225
$N_t = 0.5$	-0.3866	0.0749	0.7291
$N_t = 1$	-0.3490	-0.0034	0.7398
$N_t = 1.5$	-0.2823	-0.1400	0.7571
$R_a = 0$	-0.3700	0.0060	0.7301
$R_a = 0.3$	-0.3846	0.0527	0.7296
$R_a = 0.5$	-0.3866	0.0749	0.7291
$R_a = 1$	-0.3879	0.1251	0.7290
$L_e = 0.5$	-0.3643	0.0930	0.5055
$L_e = 1$	-0.3866	0.0749	0.7291
$L_e = 1.5$	-0.4030	0.0696	0.9021
$L_e = 2$	-0.4162	0.0681	1.0503

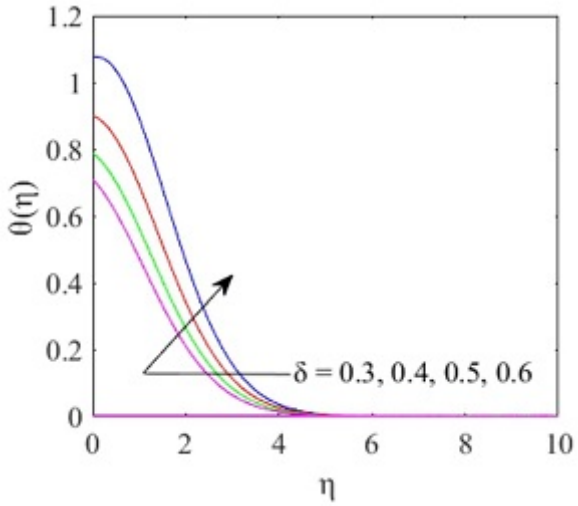

Figure 27: Temperature with η for disparate the Source/Sink facts δ.

table analyses and presents the effect of physical parameters on skin friction, local Nusselt number, and local Sherwood number. The following is a summary of the findings:

- Increasing the magnetic field parameter causes the velocity field to decrease and the temperature distribution to improve.
- The velocity and temperature field both are decrease for Prandtl number but reverse effect is seen in of radiation restriction R_a, Eckert numeral E_c, Thermophoresis limitations N_t,Brownian motion limitations N_b, Biot Numeral B_i and warmth Source/Sink δ.
- The parameter of proportion of the free stream speed to the speed of the stretching sheet λ, decrease the distribution of temperature.
- The Lewis factor decrease the distribution of concentration.
- The Permeability restriction K help to lessening the velocity arena and increase the supply of temperature arena.
- The thermal buoyancy parameter λ_1 an Solutal buoyancy parameter λ_2 help to increase the speed and decrease the temperature field.
- Sherwood number, Skin friction, and Nusselt number are increasing function of proportion of the free stream speed to the speed of the extending sheet restriction λ, Biot Number B_i, thermal buoyancy restriction λ_1 and Solutal buoyancy restriction λ_2 and decreasing function of magnetic field restriction M, Prandtl numeral P_r and Permeability restriction K.
- Skin friction and Sherwood number are increasing function of Eckert number E_c, heat Source/Sink δ, Brownian motion parameter N_b and Thermophoresis parameter N_t. But reverse effect is seen in Nusselt number.

[1] [2] [5] [6] [4] [7] [8] [9] [10] [11] [12] [13] [15] [16] [14] [18] [17] [19] [20] [21] [22] [24] [23] [25] [26] [28] [29] [30] [31] [32] [3] [27]

References

[1] Ali, B., Nie, Y., Khan, S. A., Sadiq, M. T., and Tariq, M. Finite element simulation of multiple slip effects on mhd unsteady maxwell nanofluid flow over a permeable stretching sheet with radiation and thermo-diffusion in the presence of chemical reaction. *Processes 7*, 9 (2019), 628.

[2] Babu, D. H., Ajmath, K., Venkateswarlu, B., and Narayana, P. Thermal radiation and heat source effects on mhd non-newtonian nanofluid flow over a stretching sheet. *Journal of Nanofluids 8*, 5 (2019), 1085–1092.

[3] Bilal, S., Shah, I. A., Akgül, A., Tekin, M. T., Botmart, T., Yahia, I., et al. A comprehensive mathematical structuring of magnetically effected sutterby fluid flow immersed in dually stratified medium under boundary layer approximations over a linearly stretched surface. *Alexandria Engineering Journal 61*, 12 (2022), 11889–11898.

[4] Daniel, Y. S., Aziz, Z. A., Ismail, Z., Bahar, A., and Salah, F. Slip role for unsteady mhd mixed convection of nanofluid over stretching sheet with thermal radiation and electric field. *Indian Journal of Physics 94*, 2 (2020), 195–207.

[5] Daniel, Y. S., Aziz, Z. A., Ismail, Z., and Salah, F. Impact of thermal radiation on electrical mhd flow of nanofluid over nonlinear stretching sheet with variable thickness. *Alexandria Engineering Journal 57*, 3 (2018), 2187–2197.

[6] Daniel, Y. S., Aziz, Z. A., Ismail, Z., and Salah, F. Thermal radiation on unsteady electrical mhd flow of nanofluid over stretching sheet with chemical reaction. *Journal of King Saud University-Science 31*, 4 (2019), 804–812.

[7] Dogonchi, A., and Ganji, D. Effect of cattaneo–christov heat flux on buoyancy mhd nanofluid flow and heat transfer over a stretching sheet in the presence of joule heating and thermal radiation impacts. *Indian Journal of Physics 92*, 6 (2018), 757–766.

[8] Ganesh, N. V., Kameswaran, P., Al-Mdallal, Q. M., Hakeem, A., and Ganga, B. Non-linear thermal radiative marangoni boundary layer flow of gamma al2o3 nanofluids past a stretching sheet. *Journal of Nanofluids 7*, 5 (2018), 944–950.

[9] Ghasemi, S., and Hatami, M. Solar radiation effects on mhd stagnation point flow and heat transfer of a nanofluid over a stretching sheet. *Case Studies in Thermal Engineering 25* (2021), 100898.

[10] Gireesha, B., Umeshaiah, M., Prasannakumara, B., Shashikumar, N., and Archana, M. Impact of nonlinear thermal radiation on magnetohydrodynamic three dimensional boundary layer flow of jeffrey nanofluid over a nonlinearly permeable stretching sheet. *Physica A: Statistical Mechanics and its Applications 549* (2020), 124051.

[11] Goud, B. S., Reddy, Y. D., and Rao, V. S. Thermal radiation and joule heating effects on a magnetohydrodynamic casson nanofluid flow in the presence of chemical reaction through a non-linear inclined porous stretching sheet. *Journal of Naval Architecture and Marine Engineering 17*, 2 (2020), 143–164.

[12] Gupta, S., Kumar, D., and Singh, J. Mhd mixed convective stagnation point flow and heat transfer of an incompressible nanofluid over an inclined stretching sheet with chemical reaction and radiation. *International Journal of Heat and Mass Transfer 118* (2018), 378–387.

[13] Hayat, T., Khan, W., Abbas, S., Nadeem, S., and Ahmad, S. Impact of induced magnetic field on second-grade nanofluid flow past a convectively heated stretching sheet. *Applied Nanoscience 10*, 8 (2020), 3001–3009.

[14] Hussain, S. M., Sharma, R., Seth, G. S., and Mishra, M. R. Thermal radiation impact on boundary layer dissipative flow of magneto-nanofluid over an exponentially stretching sheet. *Int. J. Heat Technol. 36*, 4 (2018), 1163–1173.

[15] Ishaq, M., Ali, G., Shah, Z., Islam, S., and Muhammad, S. Entropy generation on nanofluid thin film flow of eyring–powell fluid with thermal radiation and mhd effect on an unsteady porous stretching sheet. *Entropy 20*, 6 (2018), 412.

[16] Jamshed, W., Goodarzi, M., Prakash, M., Nisar, K. S., Zakarya, M., Abdel-Aty, A.-H., et al. Evaluating the unsteady casson nanofluid over a stretching sheet with solar thermal radiation: An optimal case study. *Case Studies in Thermal Engineering 26* (2021), 101160.

[17] Khan, S. A., Ali, B., Eze, C., Lau, K. T., Ali, L., Chen, J., and Zhao, J. Magnetic dipole and thermal radiation impacts on stagnation point flow of micropolar based nanofluids over a vertically stretching sheet: finite element approach. *Processes 9*, 7 (2021), 1089.

[18] Khan, S. A., Nie, Y., and Ali, B. Multiple slip effects on magnetohydrodynamic axisymmetric buoyant nanofluid flow above a stretching sheet with radiation and chemical reaction. *Symmetry 11*, 9 (2019), 1171.

[19] Mishra, A., and Kumar, M. Thermal performance of mhd nanofluid flow over a stretching sheet due to viscous dissipation, joule heating and thermal radiation. *International Journal of Applied and Computational Mathematics 6*, 4 (2020), 1–17.

[20] Mjankwi, M. A., Masanja, V. G., Mureithi, E. W., and James, M. N. Unsteady mhd flow of nanofluid with variable properties over a stretching sheet in the presence of thermal radiation and chemical reaction. *International Journal of Mathematics and Mathematical Sciences 2019* (2019).

[21] Mohammadein, S., Raslan, K., Abdel-Wahed, M., and Abedel-Aal, E. M. Kkl-model of mhd cuo-nanofluid flow over a stagnation point stretching sheet with nonlinear thermal radiation and suction/injection. *Results in Physics 10* (2018), 194–199.

[22] Muhammad, T., Waqas, H., Farooq, U., and Alqarni, M. Numerical simulation for melting heat transport in nanofluids due to quadratic stretching plate with nonlinear thermal radiation. *Case Studies in Thermal Engineering 27* (2021), 101300.

[23] Pal, D., Mondal, S., and Mondal, H. Entropy generation on mhd jeffrey nanofluid over a stretching sheet with nonlinear thermal radiation using spectral quasilinearisation method. *International Journal of Ambient Energy 42*, 15 (2021), 1712–1726.

[24] Pal, D., and Mondal, S. K. Mhd nanofluid bioconvection over an exponentially stretching sheet in the presence of gyrotactic microorganisms and thermal radiation. *BioNanoScience 8*, 1 (2018), 272–287.

[25] Patil, A. B., Humane, P. P., Patil, V. S., and Rajput, G. R. Mhd prandtl nanofluid flow due to convectively heated stretching sheet below the control of chemical reaction with thermal radiation. *International Journal of Ambient Energy* (2021), 1–13.

[26] Qayyum, S., Hayat, T., and Alsaedi, A. Thermal radiation and heat generation/absorption aspects in third grade magneto-nanofluid over a slendering stretching sheet with newtonian conditions. *Physica B: Condensed Matter 537* (2018), 139–149.

[27] Shah, I. A., Bilal, S., Akgül, A., Tekin, M. T., Botmart, T., Zahran, H. Y., and Yahia, I. S. On analysis of magnetized viscous fluid flow in permeable channel with single wall carbon nano tubes dispersion by executing nano-layer approach. *Alexandria Engineering Journal 61*, 12 (2022), 11737–11751.

[28] Shoaib, M., Raja, M. A. Z., Sabir, M. T., Islam, S., Shah, Z., Kumam, P., and Alrabaiah, H. Numerical investigation for rotating flow of mhd hybrid nanofluid with thermal radiation over a stretching sheet. *Scientific Reports 10*, 1 (2020), 1–15.

[29] Sithole, H., Mondal, H., and Sibanda, P. Entropy generation in a second grade magnetohydrodynamic nanofluid flow over a convectively heated stretching sheet with nonlinear thermal radiation and viscous dissipation. *Results in Physics 9* (2018), 1077–1085.

[30] Sreedevi, P., and Reddy, P. S. Combined influence of brownian motion and thermophoresis on maxwell three-dimensional nanofluid flow over stretching sheet with chemical reaction and thermal radiation. *Journal of Porous Media 23*, 4 (2020).

[31] Sreedevi, P., Sudarsana Reddy, P., and Chamkha, A. Heat and mass transfer analysis of unsteady hybrid nanofluid flow over a stretching sheet with thermal radiation. *SN Applied Sciences 2*, 7 (2020), 1–15.

[32] Sudarsana Reddy, P., and Sreedevi, P. Impact of chemical reaction and double stratification on heat and mass transfer characteristics of nanofluid flow over porous stretching sheet with thermal radiation. *International Journal of Ambient Energy* (2020), 1–11.